STEM CELLS AND DEVELOPMENT
Volume 20, Number 3, 2011

DOI: 10.1089/scd.2010.0354

Placental Perivascular Cells for Human Muscle Regeneration

Tea Soon Park,[1,2] Manuela Gavina,[1,*] Chien-Wen Chen,[1,*] Bin Sun,[1] Pang-Ning Teng,[1] Johnny Huard,[1,3,4] Bridget M. Deasy,[1,3,4] Ludovic Zimmerlin,[1] and Bruno Péault[1,3,5]

Perivascular multipotent mesenchymal progenitors exist in a variety of tissues, including the placenta. Here, we suggest that the abundant vasculature present in the human placenta can serve as a source of myogenic cells to regenerate skeletal muscle. Chorionic villi dissected from the mid-gestation human placenta were first transplanted intact into the gastrocnemius muscles of SCID/*mdx* mice, where they participated in muscle regeneration by producing myofibers expressing human dystrophin and spectrin. In vitro-cultured placental villi released rapidly adhering and migratory CD146+CD34−CD45−CD56− cells of putative perivascular origin that expressed mesenchymal stem cell markers. CD146+CD34−CD45−CD56− perivascular cells isolated and purified from the placental villi by flow cytometry were indeed highly myogenic in culture, and generated dystrophin-positive myofibers, and they promoted angiogenesis after transplantation into SCID/*mdx* mouse muscles. These observations confirm the existence of mesenchymal progenitor cells within the walls of human blood vessels, and suggest that the richly vascularized human placenta is an abundant source of perivascular myogenic cells able to migrate within dystrophic muscle and regenerate myofibers.

Introduction

The placenta is a transitory organ that develops during pregnancy at the feto-maternal interface. It consists of 3 distinct layers: the amnion and chorion, both of fetal origin, and the maternal decidua. The chorionic villous placenta contains a rich vasculature to supply oxygen and nutrients to the fetus [1–4] *via* chorionic villi that are the vascular projections structured by an outer layer of trophoblastic cells and inner part of fetal blood vessels. These numerous blood vessels result from neovascularization followed by active angiogenesis. Capillaries initially form *de novo* in the chorionic villi from hemangiogenic progenitors, which in turn engender endothelial networks through successive steps of differentiation and proliferation under the influence of trophoblast cells [5,6]. Angiogenesis continues during placentation with development of both endothelial and perivascular cells [2,7,8].

The placenta is rich in stem/progenitor cells. While the amnion has been reported to contain epiblast-derived pluripotent/multipotent stem cells (aka human amniotic epithelial cells) that express embryonic stem cell markers [4,9–14], placenta-derived mesenchymal stem cells (MSCs) have been isolated from all 3 layers (amnion [3,15,16], chorion [17–19], and decidua [3,20]). Human trophoblastic stem cells were isolated from the human villous placenta over 4 decades ago [7], and yet the most recent studies on placental MSC still rely on mundane, indirect isolation strategies, on a par with the lack of knowledge on the identity of these cells [17–19,21,22].

We previously identified microvascular pericytes as a major and ubiquitous source of human MSC in various fetal and adult organs [23], including fetal placenta. While additional cell populations may act as mesenchymal progenitors in particular tissues such as fat [24], pericytes represent an unique and consistently detectable population of cells in all organs, which express a specific set of surface antigens, including the cell adhesion molecule CD146 [25] and the proteoglycan NG2, and lack endothelial and hematopoietic cell markers. On the basis of this distinct cellular signature, we showed that pericytes can be reliably isolated as CD146+CD34−CD56−CD45− cells from various organs, including placenta [23]. Muscle-derived pericytes belong to a collection of distinct myogenic stem/progenitor cells [26–28], and efficiently regenerate skeletal muscle. Yet, pericytes exhibit robust myogenic potential independently of their tissue

[1]Stem Cell Research Center, Children's Hospital of Pittsburgh of University of Pittsburgh Medical Center, Pittsburgh, Pennsylvania.
[2]Institute for Cell Engineering, Johns Hopkins School of Medicine, Baltimore, Maryland.
[3]McGowan Institute for Regenerative Medicine, University of Pittsburgh, Pittsburgh, Pennsylvania.
[4]Department of Orthopedic Surgery, Children's Hospital of Pittsburgh of University of Pittsburgh Medical Center, Pittsburgh, Pennsylvania.
[5]Orthopaedic Hospital Research Center, David Geffen School of Medicine, University of California at Los Angeles, Los Angeles, California.
*There authors equally contributed to this work.

origin, as pericytes sorted from pancreas, adipose tissue, and placenta are also myogenic [23,25].

In the present work, we characterized in detail placenta villus cell subsets and their myogenicity. First, we documented the myogenic potential in vivo of intact, undissociated villus fragments. We then evaluated in detail the intrinsic properties of migration, adhesion, and MSC phenotype of expanded pericyte-like and nonpericyte populations. We finally compared the in vitro and in vivo myogenic potentials of freshly isolated placenta pericytes and nonpericyte populations, as well as their angiogenic capacities in vivo. Together, our findings suggest the abundant existence of highly migratory and myogenic perivascular mesenchymal progenitor cells within the placental vasculature. On the basis of these results, we propose placenta as a convenient, rich source of newly generated blood vessels suitable for cellular therapeutic applications.

Materials and Methods

Isolation of purified villous fragments from the human fetal placenta

After informed consent, in compliance with the Institutional Review Board (protocol number 0506176) at the University of Pittsburgh, placentas were obtained from midgestation (18–23 weeks) interrupted pregnancies. Bundles of chorionic anchoring (stem) villi were separated from the chorionic plate and spread out using forceps to separate individual villi from each other (Fig. 1A, b–d). The villi were washed multiple times in phosphate buffered saline (PBS; Sigma, St Louis, MO) until blood cells and tissue debris were removed (Fig. 1A, e). Terminal parts of the villi were cut off to avoid the presence of any decidual tissue (Fig. 1A, f). Dissected villi were cut into $\sim$1-mm^3 pieces (Fig. 1A, g) for in vitro culture/assay or transplantation into mouse muscles.

Immunofluorescence staining of placental blood vessels

For in toto immunofluorescence staining (Fig. 1B), dissected villi were placed on glass slides and immunostained. Villus fragments were successively incubated with unconjugated mouse anti-human CD34 (BD Biosciences, 1:100) followed by goat anti-mouse-biotin (Dako, 1:500), and streptavidin-Cy3 (Sigma, 1:500). Next, anti-CD146-FITC (AbD Serotec, 1:50) was added for 2 h at room temperature (RT). 4′,6-Diamidino-2-phenylindole (DAPI; Molecular Probes, 1:2000) was added to stain nuclei. Tissue was washed in PBS after each incubation. Photographs were captured using a Nikon Eclipse TE2000-U microscope and Snap Advanced software.

For cross-sectional staining (Fig. 1C), dissected villi were embedded in tissue freezing medium (Triangle Biomedical Sciences), frozen in liquid nitrogen vapors, cryosectioned at 6–7 μm, and immunostained, as previously described [23,29]. Frozen sections were fixed in a mixture of cooled (−20°C) methanol and acetone (1:1) for 5 min before staining. Sections were blocked using 5% goat serum for 1 h at RT and incubated overnight at 4°C with either unconjugated mouse anti-human CD34 (BD Biosciences), CD56 (BD Pharmingen), CD133 (Miltenyi Biotec), CD144 (Santa Cruz Biotechnology), CD146 (BD Biosciences), or KDR (vascular endothelial growth factor receptor-2; Santa Cruz Biotechnology, all 1:100). Then, goat anti-mouse-biotin (Dako) and streptavidin-Cy3 (Sigma) were incubated sequentially. Alternately, sections were stained in addition with anti-alpha-smooth muscle actin-FITC (αSMA; Sigma, 1:200), actin-CD31-FITC (Santa Cruz Biotechnology, 1:50), or actin-CD146-FITC (AbD Serotec) followed by DAPI staining. Photographs were captured using a Nikon Eclipse TE2000-U microscope or Olympus FLUOVIEW FV1000.

For immunocytostaining, cells grown out of placenta villi were plated in 48-well plates at 2×10^4 cells/cm^2 and fixed using a mixture of cooled (−20°C) methanol and acetone (1:1) for 5 min. Cells were then incubated overnight in unconjugated rabbit anti-human PDGF receptor-β (PDGFR-β; Santa Cruz Biotechnology), mouse anti-human NG2 (BD Biosciences), CD31 (Chemicon), CD144 (Bender MedSystems), or CD146 (BD Biosciences) (all 1:100). PDGFR-β staining was revealed using donkey anti-rabbit-Alexa 488 (Molecular Probes, 1:500) secondary antibody. For all other mouse anti-human unconjugated antibodies, cells were sequentially incubated with biotinylated goat anti-mouse (Dako) and streptavidin-Cy3 (Sigma). Additionally, some cells were costained with anti-αSMA-FITC (Dako), anti-CD34-FITC (Miltenyi Biotec, 1:50), anti-CD146-FITC (AbD Serotec), or anti–von Willebrand factor–FITC (vWF, US Biological, 1:100), followed by DAPI staining.

Villus fragment culture

Dissected villi were cultured intact on 24-well plates with or without 0.2% gelatin coating either in muscle proliferation medium (PM) containing Dulbecco's modified Eagle's medium (Invitrogen), 10% fetal calf serum (FCS, Invitrogen), 10% horse serum (Sigma), 1% chick embryo extract, and 1% penicillin/streptomycin (PS; Invitrogen), or in endothelial growth medium-2 (EGM2; Lonza). When outgrowing cells reached over 80% confluency, the villi pieces remaining intact were carefully removed, transferred into, and subsequently cultured on new gelatin-coated or noncoated plates. This procedure was repeated till the 5th outgrowth. Monolayers of outgrown cells were further expanded additional 3–5 passages in alpha-MEM (Invitrogen) supplemented with 20% FCS and 1% PS, and then used for cell sorting or analyses.

Myogenic differentiation in vivo

Four pieces of dissected villi (1 mm^3 each) were transplanted into a surgical pocket within the gastrocnemius muscle of a dystrophic SCID/*mdx* mouse. Animals were sacrificed 2 and 4 weeks after transplantation. Harvested muscles were frozen in cooled 2-methylbutane between −50°C and −60°C, and cryosectioned at 6–8 μm. Sections were fixed in a mixture of cooled (−20°C) methanol and acetone (1:1) for 5 min before staining. Nonspecific antibody binding was blocked with 5% goat serum and permeablized 0.1% Triton in PBS. Sections were incubated overnight at 4°C with mouse anti-human dystrophin (hDys3, Novocastra, 1:20), anti-spectrin (Novocastra, 1:100), anti-lamin A/C (Novocastra, 1:100), or anti-human nuclear antigen (Chemicon, 1:50) antibodies, followed by goat anti-mouse-biotin (Dako) and streptavidin-Cy3 (Sigma).

Freshly isolated CD146−CD34+CD45−CD56−, CD146+CD34−CD45−CD56−, CD146−CD34−CD45−CD56−, and unsorted cells from fetal placenta villi were injected into the

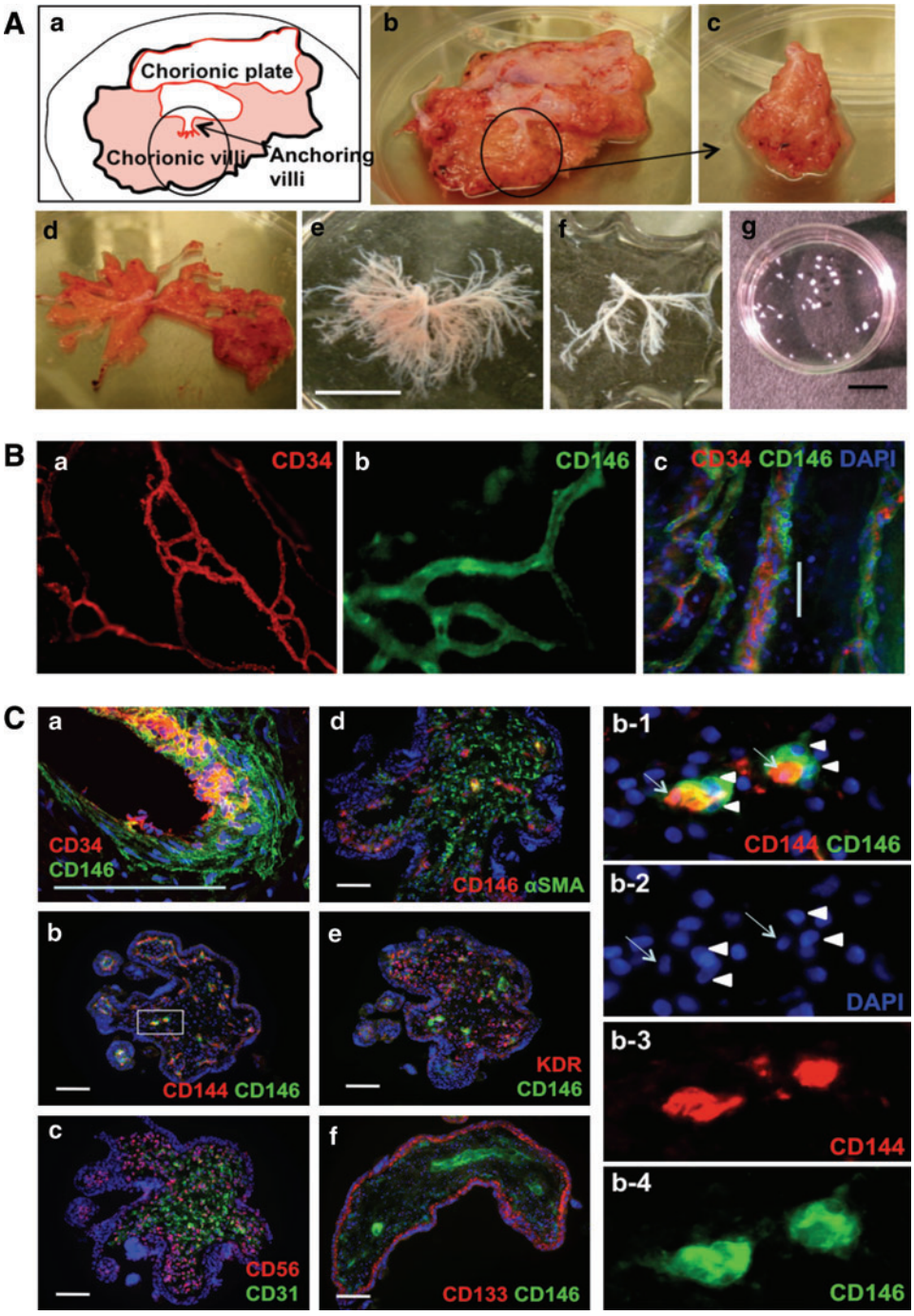

FIG. 1. Isolation and characterization of human fetal placental villi. **(A)** Isolation of chorionic villi from the 22-week placenta **(a, b)**. A portion of fetal placenta **(c**, circled in **a** and **b)** has been separated from the chorionic plate, stretched **(d)**, and washed several times in PBS **(e)**. Dissected villi **(f)** were cut into 1-mm^3 fragments **(g)** for transplantation and in vitro analysis. **(B)** In toto immunofluorescence staining of dissected placental villi. CD34+ endothelial cells **(a**, **c**, red**)** are surrounded by CD146+ perivascular cells **(b**, **c**, green**)**. **(C)** Immunofluorescence staining on cryosections of dissected placental villi. Blood vessels and capillaries are composed with endothelial cells expressing CD34 **(a**, red**)**, CD144 **(b**, red**)**, and CD31 **(c**, green**)** and perivascular cells expressing CD146 **(**green in **a**, **b**, **e**, and **f**; red in **d)** or αSMA **(d**, green**)**. Enlarged squared area in **b (b1–b4)** shows CD144+ endothelial cells (*arrows*) and CD146+ pericytes (*arrow heads*). Nonvascular cells express CD56 **(c**, red**)**, αSMA **(d**, green**)**, and KDR **(e**, red**)**. Trophoblast layers express CD133 **(f**, red**)**. Scale bars are 10 mm in **A**; 50 μm in **B** and **C**. αSMA, alpha-smooth muscle actin. Color images available online at www.liebertonline.com/scd.

gastrocnemius muscles of dystrophic SCID/*mdx* mice. Each muscle received 2×10^4 cells and was harvested 4 weeks post-transplantation. Muscles were processed as described above and stained with rabbit antidystrophin antibody (Abcam, 1:100) followed by secondary donkey anti-rabbit antibody coupled to Alexa 488 (Molecular Probes, 1:500).

Myogenic differentiation in vitro

Cells were plated at 2×10^4 cells/cm^2 in muscle PM. At 60%–70% confluence, the culture medium was half diluted in Dulbecco's modified Eagle's medium (to reduce the serum concentration). Culture medium/serum concentration was successively reduced daily until a concentration of 2% was reached. The medium was then renewed every other day until multinucleated cells were observed. Differentiated cells were fixed in cooled methanol (−20°C) for 5 min before staining. Cells were permeablized with 0.3% Triton in PBS. Mouse anti-human desmin (Sigma, 1:100) was incubated with cells overnight at 4°C. Goat anti-mouse biotin (Dako) and streptavidin-Cy3 (Sigma) were then incubated sequentially.

Flow cytometry analysis and cell sorting

Outgrown villi cells were trypsinized, washed, and stained with mouse anti-human CD44-PE (Invitrogen), CD73-PE (BD Biosciences), CD90-PE (Immunotec), CD105-PE

(Invitrogen), and CD146-FITC (AbD Serotec) (all 1:100). Each incubation was performed for 20 min at 4°C.

Alternatively, 2 g of chorionic villi was minced and suspended in 20 mL of collagenases type I, II, and IV (all at 1 mg/mL; Sigma). After a 30-min incubation on a rotating device (150 rpm) at 37°C, trypsin was added (final concentration 0.25%, Invitrogen) for another 10 min. Cells were filtered through a 70-μm cell strainer and washed free of enzymes. The cell pellet was re-suspended in red cell lysis buffer for 15 min at RT. After another centrifugation, cells were incubated for 30 min at 4°C with mouse anti-human CD34-PE (DAKO), CD56-PE-Cy7 (BD Biosciences), CD45-APC (BD Biosciences), CD146-FITC (Serotec) (all 1:50), and 7-aminoactinomycin D (7-AAD; BD Biosciences; 1:100). Cells were analyzed and sorted using a FACSAria flow cytometer (Becton-Dickinson) with FACSDiva software (Becton-Dickinson).

Migration (wound healing) assay in vitro

Cells were plated in 12-well plates at a density of 5×10^5 cells/well in α-MEM supplemented with 20% FCS, 1% PS, and cultured until confluent. A single straight wound was created in the center of the resulting monolayers using a sterile plastic pipette tip [30]. Cells were washed twice in PBS and cultured in α-MEM supplemented with 2% FCS, 1% PS to reduce proliferation. Each population was cultured in triplicate wells and photographed (3 pictures per well) at day 0 (postwound) and day 1 (24 h later). Average distance at day 0 (D_0) was calculated from the mean of 4 distances between cells on either side of the wound per picture. Average distance at day 1 (D_1) was calculated from the mean of at least 10 distinct distances between cells per picture. Migration rate (%) was calculated according to the following equation: $[(D_0 - D_1)/D_0]\times100$.

Adhesion assay

Cells were plated at 2×10^5 cells/well in 6-well plates, which were either uncoated, or precoated overnight with type I collagen, 0.2% gelatin, 2 μg/cm^2 fibronectin, or 1 mL/well undiluted FCS. One hour later, floating cells were removed and adherent cells were fixed in 1% paraformaldehyde for 15 min at RT, and then stained with DAPI (Molecular Probes). Five images were randomly captured from each well to provide the average numbers of cells attached in each condition ($n=3$).

Real-time quantitative reverse transcriptase-polymerase chain reaction

Total RNA was extracted from 2×10^4 or more cells using the Nucleospin RNA kit (Clontech). cDNA was synthesized with SuperScript™ II reverse transcriptase (Invitrogen), according to manufacturer's instructions. cDNA and primers were added to SYBR Green PCR master mix (Applied Biosystems) according to manufacturer's instructions. The quantitative analysis was performed by the Genetics Core Laboratory at the University of Pittsburgh. All data were normalized to human cyclophilin, which was used as an internal control. The primer sequences are listed in Supplementary Table S1 (Supplementary Data are available online at www.liebertonline.com/scd).

Statistics

Data are summarized as average ± standard deviation. Statistical comparison between groups was performed using 2-tailed Student's *t*-test (95% confidence interval). *P* values are listed in the figures.

Results

Isolation and characterization of placental villi

Over 20 individual placentas were used for this project. Developmental stages ranged between 17 and 23 weeks of gestation (20.4 ± 1.9 weeks, $n=18$) and weights averaged 27.1 ± 10.6 g ($n=6$). Bundles of chorionic villi attached to the chorionic plate were easily distinguishable (Fig. 1A, a, b).

Fetal blood vessels located near the surface and inside of villi were detected by in toto immunostaining, revealing the whole vascular anatomy (Fig. 1B, c) constituted of luminal endothelial CD34+ cells (Fig. 1B, a) and perivascular CD146+cells (Fig. 1B, b). Observation of immunostained villus cross sections confirmed fetal blood vessels to be composed of CD34+CD144+ endothelial cells surrounded by CD146+ perivascular cells (Fig. 1C, a, b, enlarged squared area of b shown in b1–b4). The inner part of chorionic villi contained a large number of small fetal blood vessels, stained for CD34 (1-C, a), CD144 (1-C, b), CD31 (1-C, c) (endothelial cells), and CD146 (1-C, a, b, d-f) (perivascular cells). Non-vascular cells (smooth muscle, mesenchymal, or fibroblastic cells) were diversely positive for CD56 (1-C, c), αSMA (1-C, d), and KDR (1-C, e). The outer layer of the villi is composed of 2 cell layers, the syncytiotrophoblast and cytotrophoblast, that are positively stained for CD133 (Fig. 1C, f).

Intramuscular transplantation of placental villi

As a first attempt to assess the inherent myogenic potential of human placenta blood vessels, we transplanted intact dissected villus fragments (Fig. 1A, g) into surgical pockets made in the gastrocnemius muscles of dystrophic SCID/*mdx* mice. The presence of human cells and myofibers was investigated at 2 and 4 weeks after transplantation. Observation of cross sections through host muscles revealed that human placental implants retained their native structure at 2 weeks post-transplantation (Fig. 2A–F, dashed circles). Human cells were identified inside the implants by detection of human-specific proteins, human nuclear antigen (hNA, Fig. 2E), and human lamin A/C (Fig. 2F). Human placenta participated in muscle regeneration, as assessed by the detection of human dystrophin-positive (hDys3+) myofibers not only close to the engrafted area (Fig. 2B, dashed square), but also in more distant regions, suggesting the migration of implanted human cells (Fig. 2B, lined square shown at higher magnification in 2-C).

Human myofibers detected by human dystrophin (Fig. 2G) and spectrin expression (Fig. 2H) were typically clustered and mostly small in diameter with single centered nuclei, which are distinctive features of early muscle regeneration (Fig. 2G, I). To demonstrate that these newly regenerated myofibers are truly of human origin, and not an intermediate product of cell fusion, we costained chimeric mouse muscle sections with antibodies to human-specific lamin A/C and spectrin. Human lamin A/C, shown in pink,

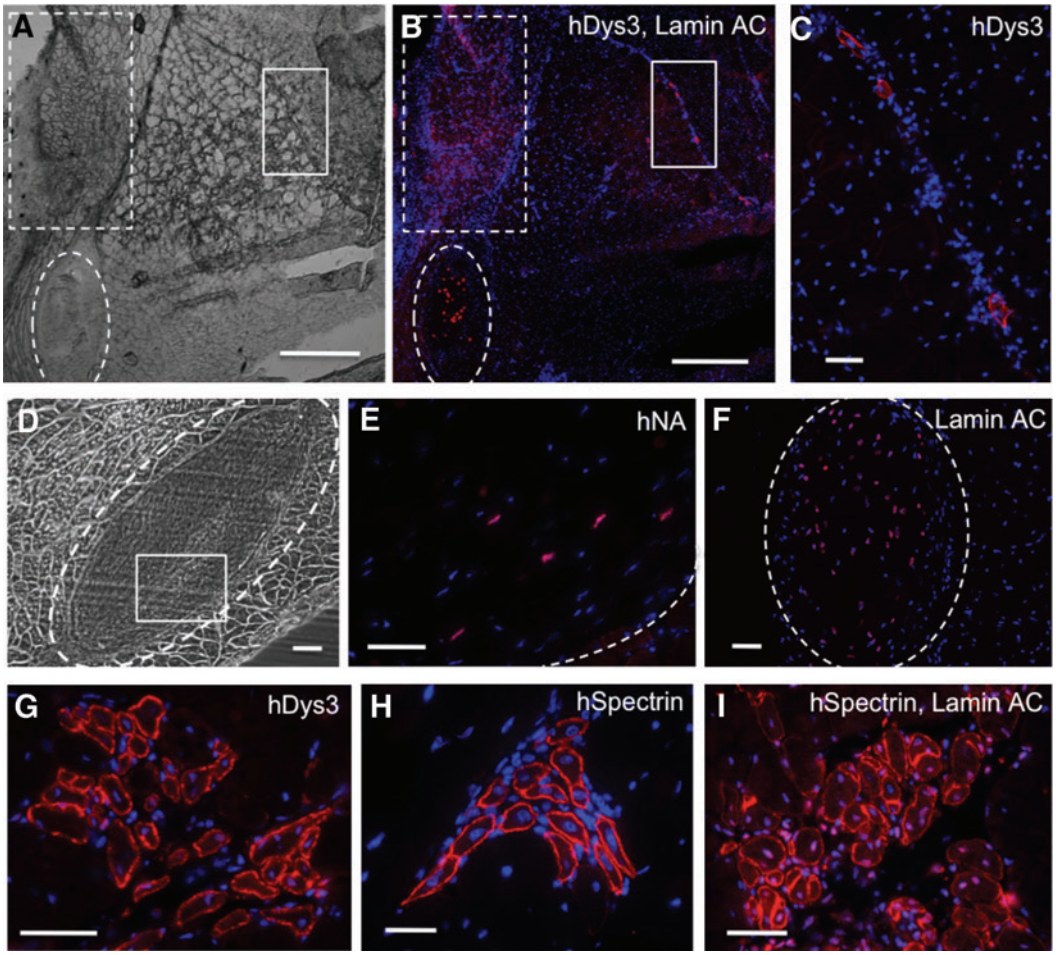

FIG. 2. Myogenicity of placenta fragments transplanted into SCID/*mdx* mouse skeletal muscles. **(A)** Bright-field picture of cross-sectioned SCID/*mdx* mouse muscle that received human placenta villi (*dashed circle*) 2 weeks earlier. **(B, C)** Immunofluorescence staining of the same section as **(A)** for human dystrophin (hDys3, red) and lamin A/C (red). The proximal region (*dashed square*) includes high numbers of hDys3+ fibers, fewer of which are present in the distal area (*lined square*, shown in **C**). **(D)** Transplantation area after 2 weeks. **(E)** Human nuclear antigen (hNA, red) detection in squared area in **D**. **(F)** Lamin A/C (red) staining of adjacent section confirms the human origin of the implant (*circled area*). **(G–I)** Immunofluorescence staining of chimeric mouse dystrophic muscle. Human myofibers generated from the transplanted human placenta fragments express human dystrophin (hDys3, **G**, red) or human spectrin (hSpectrin, **H**, red). **(I)** Staining of hSpectrin (myofiber membrane) and lamin A/C (nuclei) confirms that spectrin+ myofibers were contributed by human cells. Nuclei were stained with Dapi (blue). Scale bars are 500 μm in **A** and **B**; 50 μm in **C–I**. Color images available online at www.liebertonline.com/scd.

is colocalized in central nuclei with DAPI staining (blue), and human spectrin (red) is exclusively expressed on the sarcolemma of myofibers (Fig. 2I) [31]. SCID/*mdx* mice that underwent sham surgery without receiving human villus segments were used as negative controls, in which muscle sections did not show any positive signal after incubation with the anti-human antibodies (data not shown).

Cell outgrowth in cultures of total placental villi

After revealing the myogenic potential of total placental villi in vivo, we proceeded to explore the progenitor cell characteristics of various cell populations residing in placental villi, including CD146+ perivascular cells. Small pieces (1 mm^3) of intact placental villi (Fig. 1A, g) were cultured on gelatin-coated or noncoated plates in EGM2 or muscle PM. Tissue adherence often failed on noncoated plates but was significantly enhanced in the presence of gelatin (or collagen type IV). Five to 7 days later, outgrowth of cells was first observed, and then sustained. Replating villus fragments for additional outgrowth followed by the first outgrowth step led to faster cell outgrowing and higher proliferation on gelatin-coated plates in EGM2 than all other conditions (Supplementary Fig. S1). Cells outgrown from villus fragments in EGM2 were of polygonal morphology and proliferated rapidly (Fig. 3A, upper row; Supplementary Video S1), whereas cells outgrown in PM were spindle shaped, resembling fibroblasts (Fig. 3A, lower row).

Proliferation was measured using the live cell imaging system, a fully automatic robotic videomicroscopy system that captures images of cell growth every 12 h for 6 days. EGM2 significantly enhanced cell proliferation rate, as compared to PM (Fig. 3B). There were no major differences in growth rate between cells cultured in coated or noncoated plates. However, the addition of extracellular matrix induced the growth of different cell populations. When dissected villi

were cultured in EGM2 on gelatin-coated plates, CD146 and NG2 double-positive cells—ie, pericytes [23]—were present, which was not observed in noncoated plates (Fig. 3C). We therefore favored the outgrowth and propagation of pericytes from dissected placental villi using gelatin-coated plates and EGM2. Cells outgrown in these conditions were immunocytostained in 48-well culture plates. Most cells expressing CD146 were also positive for PDGFR-β and NG2, further indicating their perivascular origin [23,26,27,32,33]. Few CD146-positive cells expressed αSMA, and cells outgrown from villi rarely expressed the endothelial cell markers CD31, CD34, CD144, and vWF (Fig. 3D).

MSC marker expression by cultured villus cells

On the basis of our immunocharacterization of cells outgrown from placenta villi, only 2 major cell populations could emerge under our culture conditions (EGM2 in gelatin-coated plates): (1) cells expressing pericyte markers and (2) cells lacking pericyte markers. Using fluorescence-activated cell sorting (FACS), we applied our previously published gating strategy [23] to isolate both populations. Cells outgrown from placenta villi were sorted as CD146+CD34−CD45−CD56− pericytes and CD146−CD34−CD45−CD56− nonpericyte cells. As observed by immunofluorescence staining, few or no endothelial cells could be detected (Fig. 3). Similarly, hardly any CD45+ and CD56+ cells were present in our cultures. Consequently, no major cell population was excluded as per this purification strategy that allowed us to eliminate remaining endothelial and hematopoietic cells.

Thereafter, sorted CD146+CD34−CD45−CD56− (CD146+) cells and CD146−CD34−CD45−CD56− (CD146−) cells were further cultured up to passage 5 and analyzed by flow cytometry. Both populations strongly and homogeneously expressed the MSC markers CD105 and CD44. CD73 expression was detected in 57.2% and 77.4% of expanded CD146+ and CD146− cells, respectively (Fig. 4B). Yet, analysis of CD90 expression revealed a major difference between both popula-

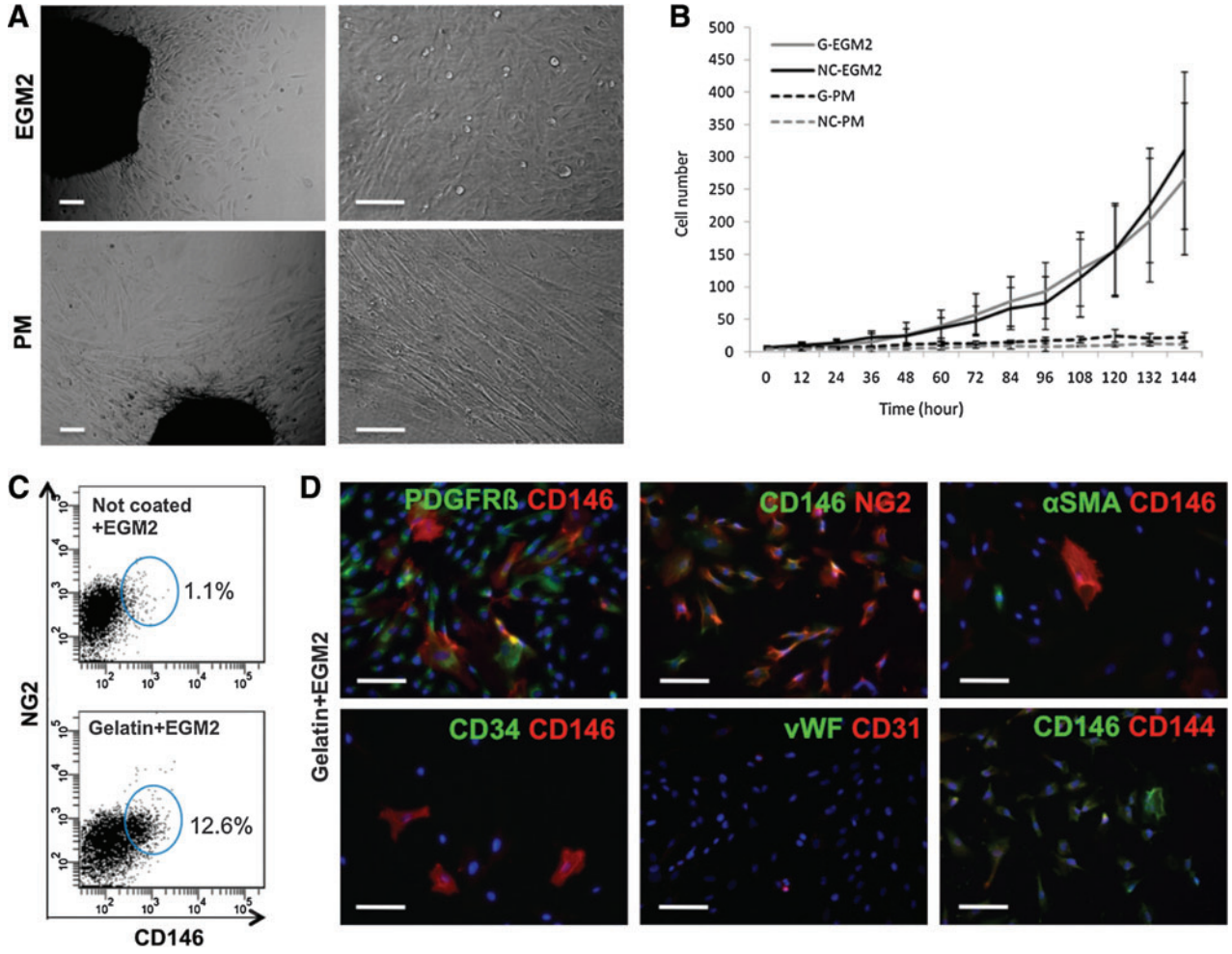

FIG. 3. In vitro outgrowth of placental villi. **(A)** Cells grown for 12 days from villus fragments exhibit different morphologies according to the culture medium used, EGM2, or muscle PM. **(B)** Proliferation measured using the Live Cell Imaging System. Cells cultured in EGM2 grow and proliferate more rapidly than those cultured in PM, whereas culture plate coating made no difference (G, gelatin; NC, not coated). **(C)** FACS analysis of out-growing cells in EGM2 medium on noncoated (*upper panel*) and gelatin-coated (*lower panel*) plates. **(D)** Immunocytostaining of cells cultured in EGM2 on gelatin-coated plates. The perivascular cell markers PDGFRβ and NG2 are coexpressed with CD146. αSMA-, CD34-, vWF-, and CD144-expressing cells were rarely observed. Scale bars in **A** and **D** are 100 μm. EGM2, endothelial growth medium-2; FACS, fluorescence-activated cell sorting; PM, proliferation medium. Color images available online at www.liebertonline.com/scd.

tions. Over 60% of CD146+ cells were positive for CD90 expression, whereas <5% of CD146− cells were (Fig. 4A, B). We examined brachyury mRNA, an early mesodermal stem cell marker, in these 2 cell populations. Higher levels of brachyury mRNA were detected in CD146+ cells (Fig. 4C, lane 2) than in CD146− cells (Fig. 4C, lane 3). GAPDH mRNA expression was used as an internal control (Fig. 4C, lanes 4 and 5).

Migration and adhesion of CD146+ and CD146− villus-derived cells

Cells outgrown from placenta villi as described above were sorted on expression of CD146 (and absence of CD34, CD45, and CD56) for further evaluation in terms of migration and adherence. CD146+, CD146−, and unsorted cells were plated and grown to over 90% confluency. A single wound was created in the center of the cell monolayer ($764 \pm 152.6\,\mu m$, $n = 12$) to observe empty space filling by migrating cells (Fig. 5A, day 0). After 24 h, CD146+ cells demonstrated quantitatively higher migratory efficiency compared to both CD146− and total unsorted cells (Fig. 5A, day 1, and 5B).

Adhesion regulates multiple aspects of cell life *via* a variety of molecules and ligands [30,34–37]. To test the behavior of villus-derived cells in the presence of different adhesion molecules, sorted CD146+ and CD146− cells were seeded on different extracellular matrix substrates. Both populations were plated, in equal numbers, onto either noncoated, FCS saturated, collagen-, gelatin-, or fibronectin-coated culture plates. One hour later, unattached cells were removed and adherent cells were counted. CD146+ cells adhered faster

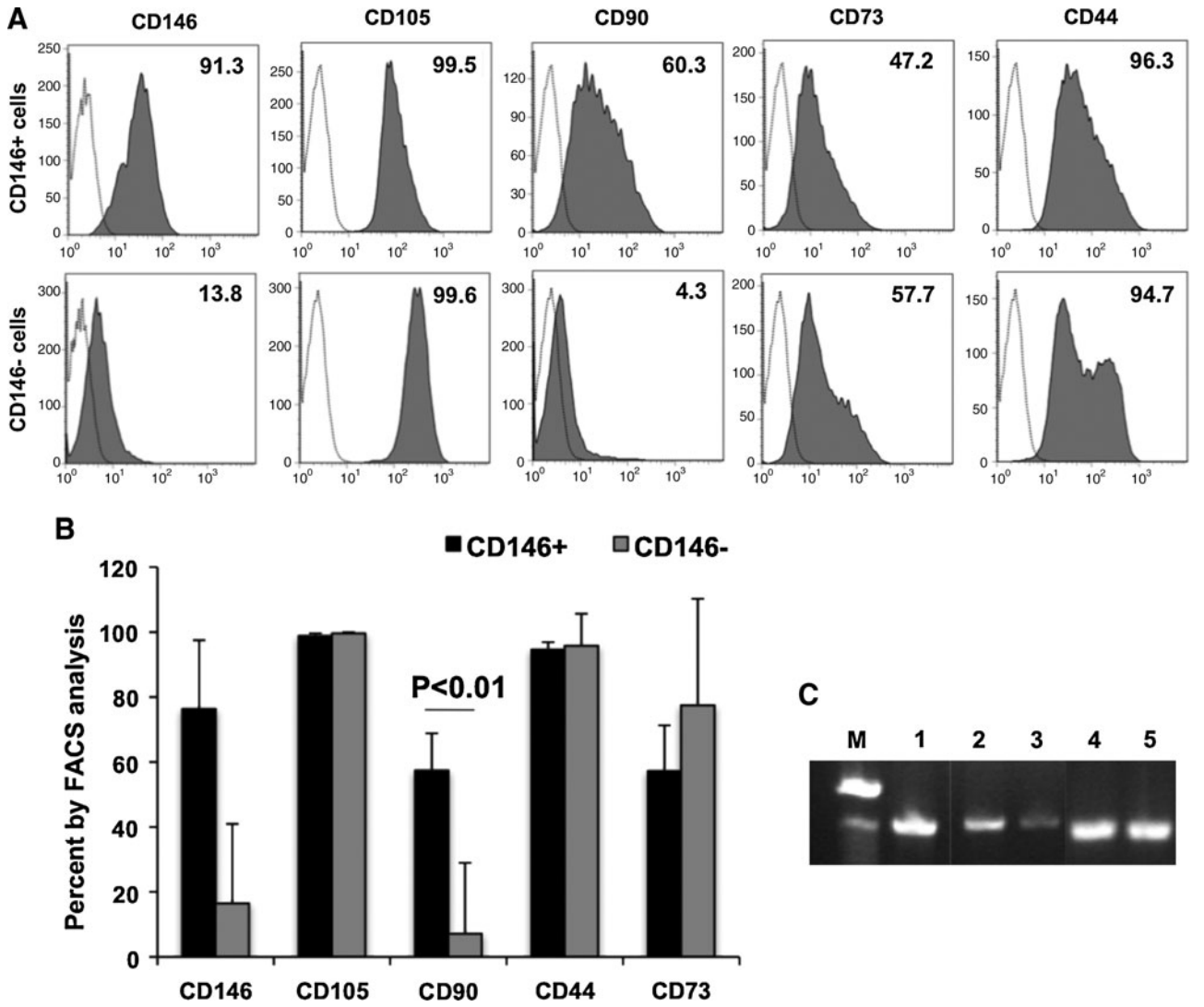

FIG. 4. MSC marker expression by cultured placental cells. **(A)** Flow cytometry analysis of CD146+CD34−CD45−CD56− (CD146+ cells, *upper row*) and CD146−CD34−CD45−CD56− (CD146− cells, *lower row*) outgrown cells for expression of MSC markers after 4 passages. Dotted lines with white background indicate isotype controls and the numbers in the histograms are percentages of antigen-expressing cells. **(B)** Average numbers of MSC marker-expressing cells within CD146+ and CD146− populations ($n = 3$). **(C)** Reverse transcriptase-polymerase chain reaction (RT-PCR) analysis of CD146+ and CD146− cells for expression of brachyury. From left: M, size marker; 1, brachyury in human fetal muscle (positive control); 2, brachyury in CD146+ cells; 3, brachyury in CD146− cells; 4, GAPDH in CD146+ cells; 5, GAPDH in CD146− cells. MSC, mesenchymal stem cell; PCR, polymerase chain reaction.

than CD146− cells to all tested extracellular coating materials: collagen, gelatin, and fibronectin. Conversely, CD146− cells attached slightly faster on noncoated plates and those saturated with FCS (Fig. 5C).

To further comprehend the distinct cell migration and adhesion properties of CD146+ cells, compared to their CD146−counterparts, we studied their expression of related genes. As assessed by real-time quantitative reverse transcriptase (RT)-polymerase chain reaction, CD146+ cells expressed integrin-alpha (Int-a) 1, 2, 4, 5, 6, integrin-beta 1 (Int-b1) and metalloproteinase-2 at higher levels than CD146− cells (Fig. 5D). Interestingly, Int-a5 (a subcomponent of the fibronectin receptor) was expressed in excess of 9-fold higher, and Int-a6 (a subcomponent of the collagen receptor) was expressed 4-fold more by CD146+ cells than CD146− cells. Strikingly, metalloproteinase-2 is expressed >25-fold higher by CD146+ cells, consistent with our observations that CD146+ cells migrate more actively than CD146− cells (Fig. 5D).

In vitro myogenesis from freshly sorted placental cells

After enzymatic digestion, placenta villus cells were purified by FACS into CD146+CD34−CD45−CD56− (CD146+ cells), CD146−CD34+CD45−CD56− (CD34+ cells), and CD146−CD34−CD45−CD56− (CD34−CD146− cells) cell populations. Villus cell suspensions included $31 \pm 11.7\%$ CD45+ hematopoietic cells ($n = 3$). After gating out CD45+ and CD56+ cells, CD34+ endothelial/adventitial cells ($3.5 \pm 2.6\%$, $n = 8$) and CD146+ perivascular cells ($1.68 \pm 0.78\%$, $n = 8$) could be clearly delineated (Fig. 6A). CD146+ CD34+CD45−CD56− endothelial cells accounted for <1% or were absent. In postsort culture, perivascular cells developed elongated cytoplasmic arms, whereas endothelial cells typically exhibited a polygonal morphology, consistent with our previous observations [23] (Fig. 6B).

Culture-expanded cells were plated at a density of 2×10^4 cells/cm^2 and cultured under conditions promoting myogenic differentiation. Fifteen days later, both CD34+ and CD146+ populations included significantly higher numbers of desmin+ cells (Fig. 6C, D) than unsorted or CD34− CD146− cells. However, the morphology of newly generated desmin+ cells differed between these populations. CD146+ cells formed elongated, occasionally multinucleated myofibers, whereas CD34+ cells generated exclusively mononucleated, scattered desmin+ cells (Fig. 6C).

To confirm the differentiation into the myogenic cell lineage, we further examined mRNA expression of CD56

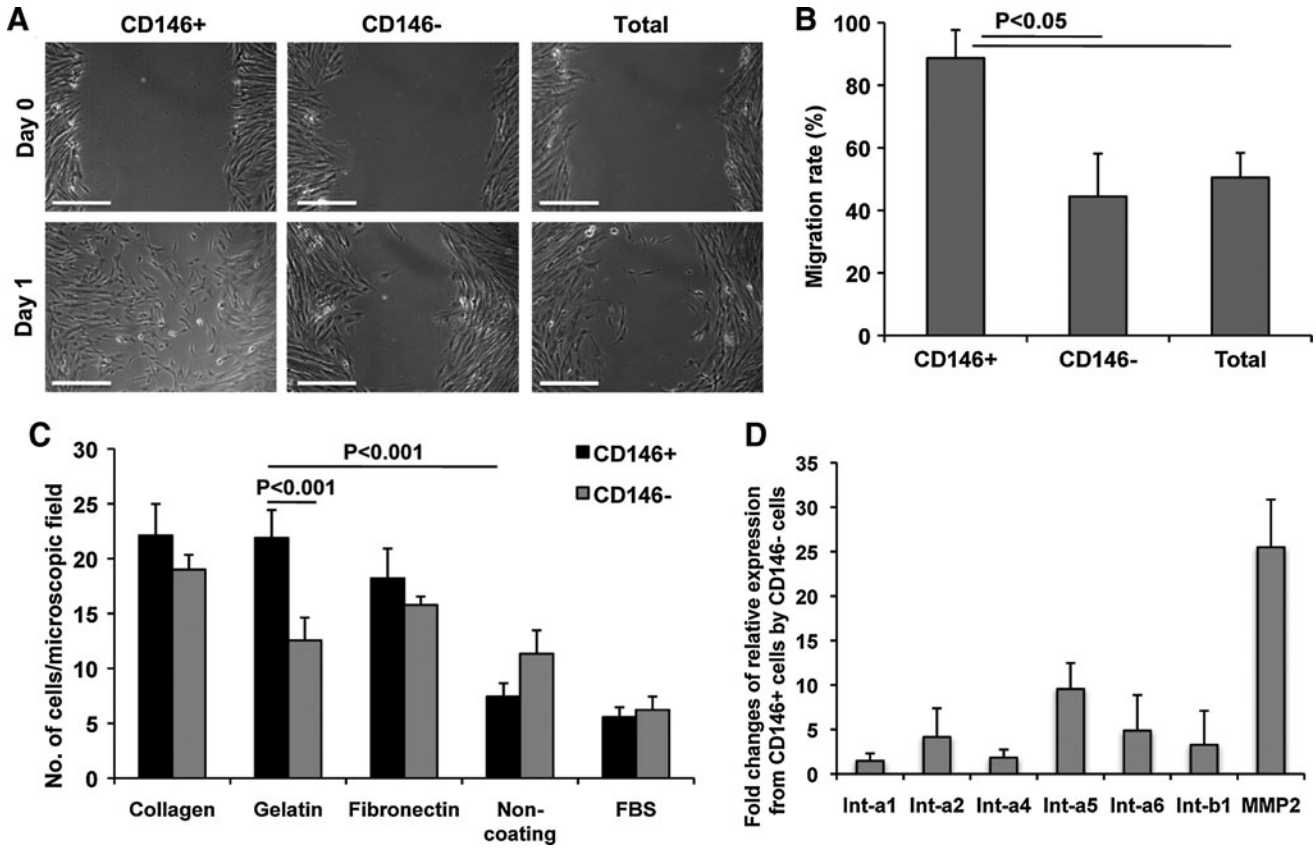

FIG. 5. Migration and adhesion of CD146+ and CD146−Cultured placental cells. **(A)** Migration/wound healing by CD146+CD34−CD45−CD56− (CD146+), CD146−CD34−CD45−CD56− (CD146−), and unsorted (total) outgrown cells. At day 0 a single wound was generated and the distances of empty space were measured at days 0 and 1. Scale bars are 500 μm. **(B)** Migration rates between distinct cell populations. Average migration rates are 88% (CD146+), 44.5% (CD146−), and 45.1% (total population), $n = 4$. **(C)** Adhesion assay on CD146+ and CD146− sorted outgrown cells using collagen-, gelatin-, fibronectin-, non-, or FBS-coated plates, $n = 8$. **(D)** Quantitative RT-PCR analysis on CD146+ and CD146− cells. Fold changes of relative mRNA expression by CD146+ to CD146− cells of, from left, integrin-alpha 1, 2, 4, 5, 6 (Int-a1, Int-a2, Int-a4, Int-a5, Int-a6), integrin-beta 1 (Int-b1), and metalloproteinase-2.

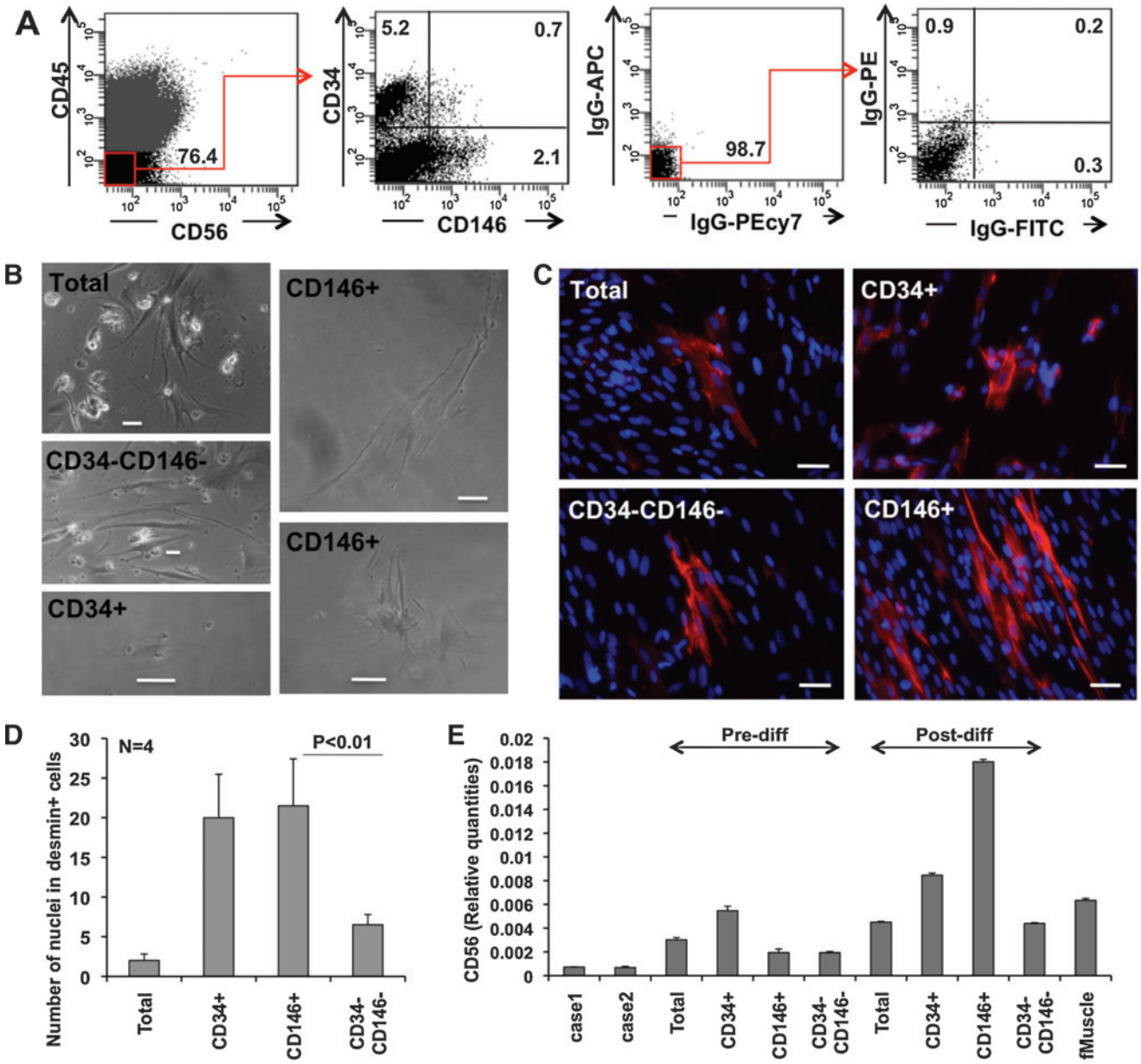

FIG. 6. In vitro myogenic differentiation of purified placental cell subsets. **(A)** Cell sorting from enzymatically digested placentae villi. After gating-out CD45+ and CD56+ cells, CD146−CD34+CD45−CD56− (CD34+), CD146+CD34−CD45−CD56− (CD146+), and CD146−CD34−CD45−CD56− (CD34−CD146−) cells were separated by FACS. Numbers in the quadrants represent percentages of cells. **(B)** FACS purified or unsorted (total) cells after 6 days in culture. **(C)** Desmin (red) expression after 15 days of myogenic differentiation. **(D)** Numbers of nuclei in desmin-positive cells after in vitro myogenic differentiation. **(E)** Quantitative RT-PCR analysis of CD56 expression in sorted populations before (Pre-differentiation) and after (Postdifferentiation) in vitro myogenic differentiation. Cases 1 and 2 indicate 2 different fetal placentas. Human fetal muscle (fMuscle, far right) was used as a positive control. Scale bars in **B** and **C** are 50 μm. Color images available online at www.liebertonline.com/scd.

(N-CAM), a commonly used marker of myoblasts [28,38–40], in vascular cells (CD34+ and CD146+), nonvascular cells (CD34−CD146−), culture-expanded unsorted cells (total), and freshly isolated unsorted cells (case 1 and case 2, representing 2 distinct donors). Human fetal muscle was used as a positive control. CD56 was upregulated after myogenic differentiation in all populations. However, CD146+ cells showed the highest CD56 expression level postdifferentiation, which was even substantially higher than in human fetal muscle (Fig. 6E, far right).

In vivo myogenesis and promotion of local angiogenesis by freshly sorted placenta cells

We next examined the myogenic and angiogenic capacities of the different freshly purified placental cell populations by injections into gastrocnemius muscles of immunodeficient dystrophic (SCID/*mdx*) mice. We injected per muscle 1×10^4 freshly sorted CD146−CD34+CD45−CD56− endothelial, CD146+CD34−CD45−CD56− perivascular, CD146−CD34−CD45−CD56− nonvascular, or unsorted (total) cells. Two

weeks postinjection, host muscles were harvested, cryosectioned, and stained with antibodies against both human and mouse dystrophin and vWF.

Both CD146+ and CD34+ sorted vascular cells generated clusters of dystrophin+ myofibers after injection into SCID/*mdx* mice. Injection of nonvascular cells only resulted in the formation of low numbers of separated single myofibers. Unsorted cells were injected as a control and gave rise to an intermediate number of myofibers, compared to vascular and nonvascular cell populations (Fig. 7A).

Tissue regeneration after injury is positively correlated with angiogenesis/neovascularization [41]. Blood vessels supply the damaged area with nutrients and oxygen, and support the migration of progenitor cells from the bone marrow or other sites [28,30,41–45]. All human cell-injected SCID/*mdx* mouse muscles contained more blood vessels than PBS-injected muscles (Fig. 7B). Interestingly, CD146+ cell injection resulted in significantly higher numbers of blood vessels than that of the other populations. Mid-gestation human fetal muscle (fMuscle) was processed in the same manner for comparison (Fig. 7C).

We have no evidence that perivascular cells could differentiate into endothelial cells in our transplantation setting. However, perivascular cells produce angiogenic factors such as basic fibroblast growth factor, heparin binding-epidermal growth factor-like growth factor (HB-EGE), keratinocyte growth factor, and vascular endothelial growth factor [25] and have the ability to organize blood vessel development from the host endothelial cells [46,47]. On the basis of published results and our own knowledge, perivascular cells promote angiogenesis *via* secretion of angiogenic factors or by recruiting domestic endothelial cells but are less likely to trans-differentiate into endothelial cells.

Discussion

Satellite cells can naturally regenerate skeletal myofibers lost to exercise, disease, or injury. Besides this well-characterized, committed muscle-residing progenitor, several multipotent mesodermal stem cells localized within skeletal muscle (myo-endothelial cells) or of broader tissue distribution (mesoangioblasts, MSCs, and pericytes) are also experimentally myogenic, although a genuine role for these cells in muscle homeostasis has not yet been demonstrated [25]. We have indeed previously observed that pericytes sorted to homogeneity by flow cytometry from multiple human organs, including the placenta, are immediately myogenic in culture or after xenogeneic transplantation into injured or diseased muscles [23].

We have now explored in much more detail the myogenic potential of human placental pericytes: first, because the naturally shed placenta is of unlimited availability as a source of therapeutic cells; second, because the abundant vasculature of placental villi can be mechanically dissected as an intact network of diversely sized blood vessels, as illustrated by Fig. 1. Successful transplantation of human placental villi under the kidney capsule of immunodeficient mice has been previously reported [48]. Here we transplanted dissected human chorionic villi intramuscularly into immunodeficient dystrophic mice, and numerous human

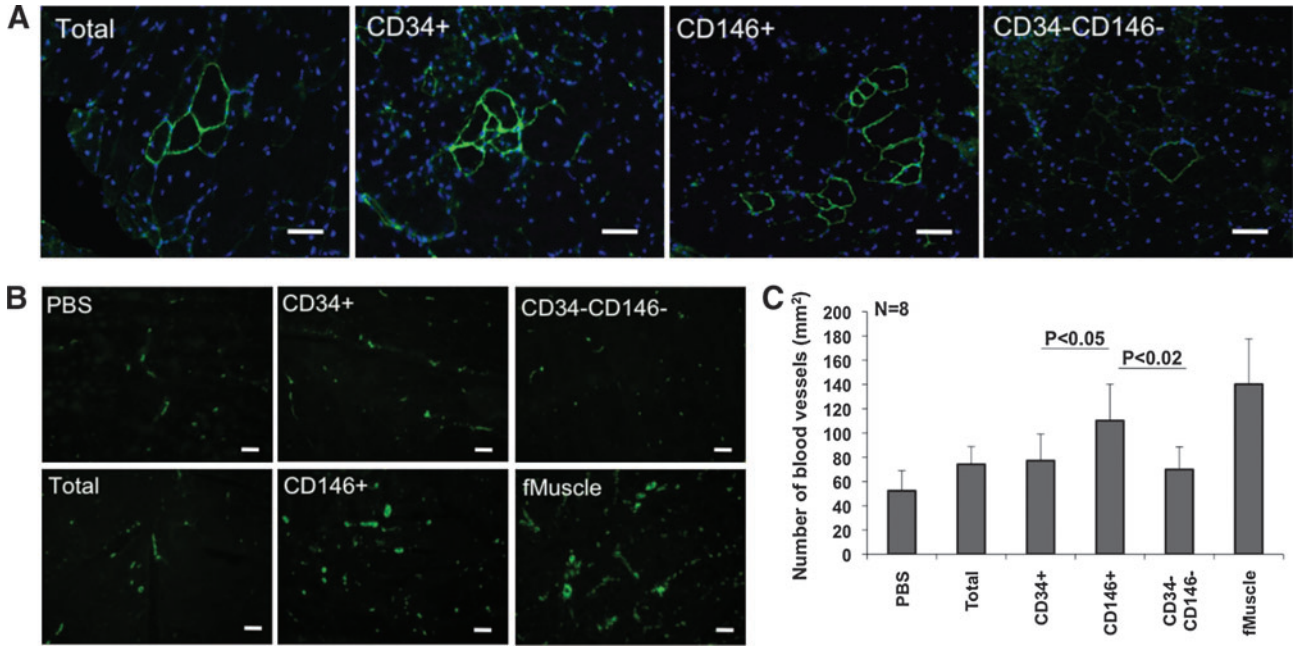

FIG. 7. Myogenesis and angiogenesis in placental cell-engrafted SCID/*mdx* mouse muscles. **(A)** Dystrophin (green) detection on frozen sections of SCID/*mdx* mouse gastrocnemius muscles that received unsorted (total), CD146−CD34+CD56−CD45− (CD34+), CD146+CD34−CD56−CD45− (CD146+), and CD146−CD34−CD56−CD45− (CD34−CD146−) freshly sorted cells. **(B)** von Willebrand factor (vWF, green) staining on frozen sections of SCID/*mdx* mouse muscles that received PBS, unsorted (Total), CD146−CD34+CD56−CD45− (CD34+), CD146+CD34−CD56−CD45− (CD146+), or CD34−CD146−CD56−CD45− (CD34−CD146−) cells. Human fetal muscle (fMuscle) was processed identically as a positive control. **(C)** Numbers of blood vessels expressing vWF in dystrophic muscles that received different human placental cells. Scale bars in **A** and **B** are 50 μm. Color images available online at www.liebertonline.com/scd.

myofibers were generated around the implants. This result is important as it shows that perivascular cells do not exhibit myogenic potential—and possibly other developmental abilities—exclusively when dissociated from adjacent endothelial cells and purified by flow cytometry [23,26]. This should be at difference with the adipogenic potential of fat tissue perivascular cells, which is inhibited by association with endothelial cells [49]. Alternatively, as an intermediate possibility, placental perivascular cells responded to the compromised muscle environment by migrating away from the endothelium, which stimulated a previously repressed myogenic potential.

Besides pericytes, did other placental cells participate in the observed myogenesis? Immunostaining of isolated placenta vessels in toto revealed the expected presence of endothelial cells and pericytes, which express CD34 and CD146, respectively. In our optimized version of the villous explant culture [50,51], 2 major cell populations grew from placental villi: pericyte-like CD146+CD34−CD45−CD56− cells and CD146−CD34−CD45−CD56− nonpericytes. CD34+, CD31+, and CD144+ endothelial cells were rapidly overgrown by these 2 cell populations. Both CD146+ and CD146− cell subsets outgrown from placental villi were sorted by FACS and further cultured separately. The pericyte origin of CD146+ cells was confirmed by their coexpression of other pericyte as well as MSC markers [23], and their multilineage mesodermal developmental potential (Supplementary Fig. S2). On the basis of these observations, and their high level of brachyury mRNA expression, CD146+ pericyte-like cells grown from placental villi appeared to be closely related to bone marrow-MSC [52], and likely represent the myogenic cell contingent evidenced in the above described transplantation experiments. To further document the affiliation of these cultured cells, both CD146+CD34−CD45−CD56− and CD146−CD34−CD45−CD56− cells—as well as CD146−CD34+CD45−CD56− cells—were detected and sorted by FACS from the native placenta and injected intramuscularly into immunodeficient dystrophic mice.

Perivascular (CD146+CD34−CD45−CD56−) and, to a far lesser extent, CD146−CD34+CD45−CD56− cells gave rise to differentiated dystrophin-expressing myofibers in the immunodeficient hosts, but only limited numbers of human myofibers were produced by CD146−CD34−CD45−CD56− cells, confirming the observations made on cultured villus blood vessels. Not only were placenta pericytes myogenic, they also significantly improved local angiogenesis, in agreement with the observation that multipotent placental MSCs (hPMSCs) can be isolated from term human placenta that are angiogenic [53]. This further suggests that MSCs and their ancestors can also mediate tissue repair by secreting growth factors [22].

The results reported here confirm and extend our conclusions regarding the existence in human organs of pericytes endowed with multilineage mesodermal potential, at the origin of MSCs once culture-adapted [23,25,33,54]. Clearly, the CD146+CD34−CD45−CD56− pericytes described around placental microvessels have a definitive advantage over neighboring cell populations in terms of growth and migration in vitro, and are the most potent as regard myogenicity. Pericytes are not, however, the only myogenic cells present in human placenta, as we have also detected power to generate myofibers within CD146−CD34+CD45−CD56− cells. Most likely, these latter cells belong to the pool of perivascular MSC ancestors of the same phenotype we have recently identified in the tunica adventitia of human arteries and veins as the stem cell equivalents in larger vessels of microvascular pericytes (Corselli et al., submitted for publication). We show in essence that the richly vascularized placenta is a convenient and abundant source of blood vessel associated stem cells.

Acknowledgments

We thank Dr. Baohong Cao for his initial support and inspiration of this project. We also thank Drs. Louis Casteilla and Toshio Miki for technical advice and guidance, and Dr. Mirko Corselli for helps with immunohistostaining. We are indebted to Alison Logar for her assistance with FACS. This study was financially supported by the Children's Hospital of Pittsburgh, McGowan Institute for Regenerative Medicine, and National Institutes of Health.

Author Disclosure Statement

No competing financial interests exist.

References

1. Turner. (1872). Observations on the structure of the human placenta. J Anat Physiol 7:120–380.
2. Strauss F. (1964). [Structure and function of the human placenta.] Bibl Gynaecol 28:3–29.
3. In't Anker PS, SA Scherjon, C Kleijburg-van der Keur, GM de Groot-Swings, FH Claas, WE Fibbe and HH Kanhai. (2004). Isolation of mesenchymal stem cells of fetal or maternal origin from human placenta. Stem Cells 22:1338–1345.
4. Miki T, T Lehmann, H Cai, DB Stolz and SC Strom. (2005). Stem cell characteristics of amniotic epithelial cells. Stem Cells 23:1549–1559.
5. Huppertz B and LL Peeters. (2005). Vascular biology in implantation and placentation. Angiogenesis 8:157–167.
6. Demir R, UA Kayisli, S Cayli and B Huppertz. (2006). Sequential steps during vasculogenesis and angiogenesis in the very early human placenta. Placenta 27:535–539.
7. Pattillo RA, GO Gey, E Delfs and RF Mattingly. (1968). *In vitro* identification of the trophoblastic stem cell of the human villous placenta. Am J Obstet Gynecol 100:582–588.
8. Kaufmann P, J Stark and HE Stegner. (1977). The villous stroma of the human placenta. I. The ultrastructure of fixed connective tissue cells. Cell Tissue Res 177:105–121.
9. Prusa AR and M Hengstschlager. (2002). Amniotic fluid cells and human stem cell research: a new connection. Med Sci Monit 8:RA253–RA257.
10. Prusa AR, E Marton, M Rosner, G Bernaschek and M Hengstschlager. (2003). Oct-4-expressing cells in human amniotic fluid: a new source for stem cell research? Hum Reprod 18:1489–1493.
11. Tamagawa T, I Ishiwata and S Saito. (2004). Establishment and characterization of a pluripotent stem cell line derived from human amniotic membranes and initiation of germ layers *in vitro*. Hum Cell 17:125–130.
12. Miki T and SC Strom. (2006). Amnion-derived pluripotent/multipotent stem cells. Stem Cell Rev 2:133–142.
13. De Coppi P, G Bartsch Jr., MM Siddiqui, T Xu, CC Santos, L Perin, G Mostoslavsky, AC Serre, EY Snyder, JJ Yoo, ME Furth, S Soker and A Atala. (2007). Isolation of amniotic

stem cell lines with potential for therapy. Nat Biotechnol 25:100–106.
14. Miki T, K Mitamura, MA Ross, DB Stolz and SC Strom. (2007). Identification of stem cell marker-positive cells by immunofluorescence in term human amnion. J Reprod Immunol 75:91–96.
15. Portmann-Lanz CB, A Schoeberlein, A Huber, R Sager, A Malek, W Holzgreve and DV Surbek. (2006). Placental mesenchymal stem cells as potential autologous graft for pre- and perinatal neuroregeneration. Am J Obstet Gynecol 194:664–673.
16. Alviano F, V Fossati, C Marchionni, M Arpinati, L Bonsi, M Franchina, G Lanzoni, S Cantoni, C Cavallini, F Bianchi, PL Tazzari, G Pasquinelli, L Foroni, C Ventura, A Grossi and GP Bagnara. (2007). Term amniotic membrane is a high throughput source for multipotent mesenchymal stem cells with the ability to differentiate into endothelial cells *in vitro*. BMC Dev Biol 7:11.
17. Igura K, X Zhang, K Takahashi, A Mitsuru, S Yamaguchi and TA Takashi. (2004). Isolation and characterization of mesenchymal progenitor cells from chorionic villi of human placenta. Cytotherapy 6:543–553.
18. Zhang X, A Mitsuru, K Igura, K Takahashi, S Ichinose, S Yamaguchi and TA Takahashi. (2006). Mesenchymal progenitor cells derived from chorionic villi of human placenta for cartilage tissue engineering. Biochem Biophys Res Commun 340:944–952.
19. Poloni A, V Rosini, E Mondini, G Maurizi, S Mancini, G Discepoli, S Biasio, G Battaglini, E Berardinelli, F Serrani and P Leoni. (2008). Characterization and expansion of mesenchymal progenitor cells from first-trimester chorionic villi of human placenta. Cytotherapy 10:690–697.
20. Strakova Z, M Livak, M Krezalek and I Ihnatovych. (2008). Multipotent properties of myofibroblast cells derived from human placenta. Cell Tissue Res 332:479–488.
21. Battula VL, S Treml, H Abele and HJ Buhring. (2008). Prospective isolation and characterization of mesenchymal stem cells from human placenta using a frizzled-9-specific monoclonal antibody. Differ Res Biol Divers 76:326–336.
22. Brooke G, H Tong, JP Levesque and K Atkinson. (2008). Molecular Trafficking Mechanisms of Multipotent Mesenchymal Stem Cells Derived from Human Bone Marrow and Placenta. Stem cells and development.
23. Crisan M. (2008). A perivascular origin for mesenchymal stem cells in multiple human organs. Cell Stem Cell 3:301–313.
24. Zimmerlin L, VS Donnenberg, ME Pfeifer, EM Meyer, B Peault, JP Rubin and AD Donnenberg. (2009). Stromal vascular progenitors in adult human adipose tissue. Cytometry A 77:22–30.
25. Chen CW, E Montelatici, M Crisan, M Corselli, J Huard, L Lazzari and B Peault. (2009). Perivascular multi-lineage progenitor cells in human organs: regenerative units, cytokine sources or both? Cytokine Growth Factor Rev 20:429–434.
26. Dellavalle A, M Sampaolesi, R Tonlorenzi, E Tagliafico, B Sacchetti, L Perani, A Innocenzi, BG Galvez, G Messina, R Morosetti, S Li, M Belicchi, G Peretti, JS Chamberlain, WE Wright, Y Torrente, S Ferrari, P Bianco and G Cossu. (2007). Pericytes of human skeletal muscle are myogenic precursors distinct from satellite cells. Nat Cell Biol 9:255–267.
27. Peault B, M Rudnicki, Y Torrente, G Cossu, JP Tremblay, T Partridge, E Gussoni, LM Kunkel and J Huard. (2007). Stem and progenitor cells in skeletal muscle development, maintenance, and therapy. Mol Ther 15:867–877.
28. Zheng B, B Cao, M Crisan, B Sun, G Li, A Logar, S Yap, JB Pollett, L Drowley, T Cassino, B Gharaibeh, BM Deasy, J Huard and B Peault. (2007). Prospective identification of myogenic endothelial cells in human skeletal muscle. Nat Biotechnol 25:1025–1034.
29. Park TS, ET Zambidis, JL Lucitti, A Logar, BB Keller and B Peault. (2008). Human embryonic stem cell-derived hematoendothelial progenitors engraft chicken embryos. Exp Hematol 37:31–41.
30. Kang Y, F Wang, J Feng, D Yang, X Yang and X Yan. (2006). Knockdown of CD146 reduces the migration and proliferation of human endothelial cells. Cell Res 16:313–318.
31. Chan J, K O'Donoghue, M Gavina, Y Torrente, N Kennea, H Mehmet, H Stewart, DJ Watt, JE Morgan and NM Fisk. (2006). Galectin-1 induces skeletal muscle differentiation in human fetal mesenchymal stem cells and increases muscle regeneration. Stem Cells 24:1879–1891.
32. Hughes S and T Chan-Ling. (2004). Characterization of smooth muscle cell and pericyte differentiation in the rat retina *in vivo*. Investig Ophthalmol Vis Sci 45:2795–2806.
33. Covas DT, RA Panepucci, AM Fontes, WA Silva Jr., MD Orellana, MC Freitas, L Neder, AR Santos, LC Peres, MC Jamur and MA Zago. (2008). Multipotent mesenchymal stromal cells obtained from diverse human tissues share functional properties and gene-expression profile with CD146+ perivascular cells and fibroblasts. Exp Hematol 36:642–654.
34. Angers-Loustau A, JF Cote and ML Tremblay. (1999). Roles of protein tyrosine phosphatases in cell migration and adhesion. Biochem Cell Biol 77:493–505.
35. Shih IM. (1999). The role of CD146 (Mel-CAM) in biology and pathology. J Pathol 189:4–11.
36. Caceres M, R Hidalgo, A Sanz, J Martinez, P Riera and PC Smith. (2008). Effect of platelet-rich plasma on cell adhesion, cell migration, and myofibroblastic differentiation in human gingival fibroblasts. J Periodontol 79:714–720.
37. Mousa SA. (2008). Cell adhesion molecules: potential therapeutic & diagnostic implications. Mol Biotechnol 38:33–40.
38. Knudsen KA, SA McElwee and L Myers. (1990). A role for the neural cell adhesion molecule, NCAM, in myoblast interaction during myogenesis. Dev Biol 138:159–168.
39. Belles-Isles M, R Roy, G Dansereau, M Goulet, B Roy, JP Bouchard and JP Tremblay. (1993). Rapid selection of donor myoblast clones for muscular dystrophy therapy using cell surface expression of NCAM. Eur J Histochem 37:375–380.
40. Stewart JD, TL Masi, AE Cumming, GM Molnar, BM Wentworth, K Sampath, JM McPherson and PC Yaeger. (2003). Characterization of proliferating human skeletal muscle-derived cells *in vitro*: differential modulation of myoblast markers by TGF-beta2. J Cell Physiol 196:70–78.
41. Deasy BM, JM Feduska, TR Payne, Y Li, F Ambrosio and J Huard. (2009). Effect of VEGF on the regenerative capacity of muscle stem cells in dystrophic skeletal muscle. Mol Ther 17:1788–1798.
42. Deasy BM, RJ Jankowski and J Huard. (2001). Muscle-derived stem cells: characterization and potential for cell-mediated therapy. Blood Cells Mol Dis 27:924–933.
43. Cao B, BM Deasy, J Pollett and J Huard. (2005). Cell therapy for muscle regeneration and repair. Phys Med Rehabil Clin N Am 16:889–907, viii.
44. Collett GD and AE Canfield. (2005). Angiogenesis and pericytes in the initiation of ectopic calcification. Circ Res 96:930–938.
45. Invernici G, C Emanueli, P Madeddu, S Cristini, S Gadau, A Benetti, E Ciusani, G Stassi, M Siragusa, R Nicosia, C

Peschle, U Fascio, A Colombo, T Rizzuti, E Parati and G Alessandri. (2007). Human fetal aorta contains vascular progenitor cells capable of inducing vasculogenesis, angiogenesis, and myogenesis *in vitro* and in a murine model of peripheral ischemia. Am J Pathol 170:1879–1892.
46. Yang YI, HI Kim, MY Choi, SH Son, MJ Seo, JY Seo, WH Jang, YC Youn, KJ Choi, SH Cheong and J Shelby. (2010). *Ex vivo* organ culture of adipose tissue for *in situ* mobilization of adipose-derived stem cells and defining the stem cell niche. J Cell Phys 224:807–816.
47. Maier CL, BR Shepherd, T Yi and JS Pober. (2010). Explant outgrowth, propagation and characterization of human pericytes. Microcirculation 17:367–380.
48. Albihn A, RO Waelchli, J Samper, JG Oriol, BA Croy and KJ Betteridge. (2003). Production of capsular material by equine trophoblast transplanted into immunodeficient mice. Reproduction 125:855–863.
49. Rajashekhar G, DO Traktuev, WC Roell, BH Johnstone, S Merfeld-Clauss, B Van Natta, ED Rosen, KL March and M Clauss. (2008). IFATS collection: Adipose stromal cell differentiation is reduced by endothelial cell contact and paracrine communication: role of canonical Wnt signaling. Stem Cells 26:2674–2681.
50. Genbacev O, SA Schubach and RK Miller. (1992). Villous culture of first trimester human placenta—model to study extravillous trophoblast (EVT) differentiation. Placenta 13:439–461.
51. Newby D, L Marks, F Cousins, E Duffie and F Lyall. (2005). Villous explant culture: characterization and evaluation of a model to study trophoblast invasion. Hypertens Pregnancy 24:75–91.
52. Dominici M, K Le Blanc, I Mueller, I Slaper-Cortenbach, F Marini, D Krause, R Deans, A Keating, D Prockop and E Horwitz. (2006). Minimal criteria for defining multipotent mesenchymal stromal cells. International Society for Cellular Therapy position statement. Cytotherapy 8:315–317.
53. Lee MY, JP Huang, YY Chen, JD Aplin, YH Wu, CY Chen, PC Chen and CP Chen. (2009). Angiogenesis in differentiated placental multipotent mesenchymal stromal cells is dependent on integrin alpha5beta1. PLoS ONE 4:e6913.
54. da Silva Meirelles L, AI Caplan and NB Nardi. (2008). In Search of the *in vivo* Identity of Mesenchymal Stem Cells. Stem Cells 26:2287–2299.

Address correspondence to:
Prof. Bruno Péault
Orthopaedic Hospital Research Center
David Geffen School of Medicine
University of California at Los Angeles
615 Charles E. Young Drive South
Los Angeles, CA 90095-7358

E-mail: bpeault@mednet.ucla.edu

Received for publication August 20, 2010
Accepted after revision October 5, 2010
Prepublished on Liebert Instant Online October 5, 2010